Inorganic Chemistry
Article

Inorg. Chem. **2010**, *49*, 11463–11472 **11463**
DOI: 10.1021/ic101437h

Stable and Tunable Phosphorescent Neutral Cyclometalated Au(III) Diaryl Complexes

Jai Anand Garg, Olivier Blacque, Thomas Fox, and Koushik Venkatesan*

Institute of Inorganic Chemistry, University of Zürich, Winterthurerstrasse 190, CH-8057, Zürich, Switzerland

Received July 19, 2010

A series of novel luminescent cyclometalated Au(III) neutral complexes of the type *cis*-[(N^C)AuL] [N^C = 2-phenylpyridine (*ppy*), L = 1,1′-biphenyl (**1**)] and *cis*-[(N^C)AuL$_2$] [N^C = 2-phenylpyridine (*ppy*), L = C_6H_5 (**2**), C_6F_5 (**3**), C_6H_4-CF_3-*p* (**4**), 2-C_4H_3S (**5**)]; [N^C = 2-(2-thienyl)pyridine (*thpy*), L = C_6H_5 (**6**), C_6F_5 (**7**)]; [N^C = 2-(5-methyl-2-thienyl)pyridine (*5 m-thpy*), L = C_6F_5 (**8**)] were successfully synthesized. The X-ray crystal structures of all compounds except **3** have been determined. These complexes were found to show long-lived emission in solution at room temperature. The emission origins of the complexes have been tentatively assigned to be derived from triplet states predominantly bearing intraligand (IL) character with some perturbation from the metal center. Density functional theory (DFT) calculations were performed to evaluate the stability associated with the complexes and TD-DFT calculations to ascertain the nature of the excited state. Variation of the cyclometalated ligands in the complexes readily leads to the tuning of the nature of the lower energy emissive states.

Introduction

The search for tunable room-temperature phosphorescent neutral metal complexes has gained tremendous impetus following the near-commercialization of cyclometalated Ir(III) complexes as OLEDs.[1−4] Recently, interest in understanding the basic photoluminescence (PL) properties of previously under-explored Au(III) complexes has gained attention with a long-term vision of using them as efficient small molecule phosphors.[5] Although, gold is significantly a "heavy-metal" with spin−orbit coupling constant $\zeta = 5100\ cm^{-1}$ for its 5d electrons,[6,7] thermally accessible, low-lying metal-centered (d-d) states and the photoreactivity exhibited by these complexes are perhaps much to the disfavor of the metal being considered for OLED applications.[8−10] However, early report of a cationic diimine Au(III) complex[9] and more recently biscyclometalated complexes of the type [Au(C^N^C)L] where L = aryl alkynyl[11,12] as well as [Au(C^N^C)(NHC)]-[PF_6][13] has led to the cognition that strong σ-donating ligands are key for populating the emissive states and also for reducing the electrophilicity at the Au(III) metal center. We hypothesized that cyclometalation, by the way of employing strong field aromatic stabilized carbanions as ligands, would sufficiently destabilize the metal centered (MC) transition to higher energies thereby creating a conducive metal−ligand environment for effective mixing of singlet−triplet states and radiative relaxation from the triplet manifold.

Pertinent to our aim of creating Au(III) complexes enriched with gold−carbon bonds and evaluating their photophysical properties, methods for the syntheses of di- or triaryl Au(III) complexes were of interest. Vicente and co-workers have reported extensive investigations, notably devoted toward development of synthetic methodologies for the creation of diaryl Au(III) complexes.[14−38] Triaryl Au(III) complexes are relatively less common, nevertheless, not completely unknown;

*To whom correspondence should be addressed. E-mail: venkatesan.koushik@aci.uzh.ch.

(1) Baldo, M. A.; O'Brien, D. F.; You, Y.; Shoustikov, A.; Sibley, S.; Thompson, M. E.; Forrest, S. R. *Nature* **1998**, *395*, 151–154.
(2) Yersin, H. *Highly efficient OLEDs with Phosphorescent Materials*; Wiley-VCH: Weinheim, 2008.
(3) Nazeeruddin, M. K.; Grätzel, M. *Struct. Bonding* (*Berlin*) **2007**, *123*, 113–175.
(4) Chou, P.-T.; Chi, Y. *Chem.—Eur. J.* **2007**, *13*, 380–395.
(5) Wong, K. M.-C.; Zhu, X. L.; Hung, L.-L.; Zhu, N. Y.; Yam, V. W.-W.; Kwok, H.-S. *Chem. Commun.* **2005**, 2906–2908.
(6) Griffith, J. S. *The Theory of Transition Metals*; Cambridge University Press: Cambridge, 1964.
(7) Gao, L.; Partyka, D. V.; Updegraff, J. B.; Deligonul, N.; Gray, T. G. *Eur. J. Inorg. Chem.* **2009**, 2711–2719.
(8) Vogler, A.; Kunkely, H. *Coord. Chem. Rev.* **2001**, *211*, 223–233.
(9) Yam, V. W.-W.; Choi, S. W.-K.; Lai, T.-F.; Lee, W.-K. *J. Chem. Soc., Dalton Trans.* **1993**, 1001–1002.
(10) Chan, C.-W.; Wong, W.-T.; Che, C.-M. *Inorg. Chem.* **1994**, *33*, 1266–1272.
(11) Wong, K. M.-C.; Hung, L.-L.; Lam, W. H.; Zhu, N. Y.; Yam, V. W.-W. *J. Am. Chem. Soc.* **2007**, *129*, 4350–4365.
(12) Yam, V. W.-W.; Wong, K. M.-C.; Hung, L.-L.; Zhu, N. Y. *Angew. Chem., Int. Ed.* **2005**, *44*, 3107–3110.
(13) Au, V. K.-M.; Wong, K. M.-C.; Zhu, N. Y.; Yam, V. W.-W. *J. Am. Chem. Soc.* **2009**, *131*, 9076–9085.
(14) Usón, R.; Laguna, A.; Vicente, J. *J. Organomet. Chem.* **1975**, *86*, 415–421.
(15) Usón, R.; Laguna, A.; Vicente, J. *J. Organomet. Chem.* **1977**, *131*, 471–475.
(16) Usón, R.; Laguna, A.; Vicente, J.; García, J.; Bergareche, B.; Brun, P. *Inorg. Chim. Acta* **1978**, *28*, 237–243.

Published on Web 11/12/2010

interesting transmetallating procedures using organomercurials have been reported by the same group for obtaining such complexes.[39−43] It is therefore of interest to investigate these established classes of complexes as potential photoactive materials.

Our initial experiments to substitute halides in monocyclometalated Au(III) complexes using lithiated aryls were promising and encouraged us to proceed further in these lines. However, we noticed that some of these complexes showed signs of decomposition during reaction and in solid state after isolation. Complexes with two aryl ligands disposed *cis* to each other in a square planar environment could be unstable because of their ability for facile reductive elimination either forming Au(I) species or metallic gold;[10,39,44−46] this could also be understood in light of the fact that Au(III) complexes tend to have large positive redox potentials. The instability could also be reminiscent to the phenomenon of Aryl/PPh_3 "*transphobia*" commonly used in palladium chemistry.[47,48] We thought that utilization of aryl ligands bearing fluorinated substituents could render the Au(III) complexes stable because of the possible increase in the π-back-donation from the metal. Indeed, in our case, complexes synthesized with such substituents were found to be more stable.

Scheme 1

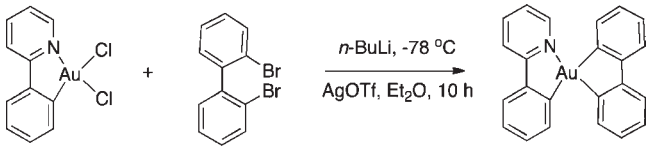

A 1

Results and Discussion

Syntheses and Characterization of Complexes. Our initial aim was to synthesize a planar (π-delocalized) cyclometalated complex using dicarbanionic chelate like 2,2′-biphenyl dianion as an ancillary ligand and evaluate its PL properties. We hoped that incorporation of biphenyl ligand would create appropriately placed intermediate electronic states below the dissociative MC states leading to interesting photophysical properties. Lithium-halogen exchange was adopted to be a general synthetic protocol for generating aryl anions suitable to substitute gold halides at low temperatures (−78 °C). Creation of complex **1** (Scheme 1) was realized with difficulty overcoming synthetic impediments to the best of 12% yield following some optimization experiments. Addition of catalytic amount of AgOTf significantly aided the formation of desired product. It needs to be mentioned here that the desired product could possibly be obtained following a transmetalation sequence described in literature and was not investigated by us.[17] Much to our encouragement the complex showed room temperature (RT) phosphorescence in fluid medium. In efforts to further improve the yield, we surmised that complexes bearing aryl carbanions as ligands but having less constrained arrangement around the metal center can be a better alternative and may exhibit better properties. Also, from a mechanistic standpoint, ligand substitution in square planar Au(III) complexes (d^8 systems) as in our case is likely to follow an associative pathway by a stepwise nucleophilic substitution sequence leading to a five coordinated ionic square planar or trigonal bipyrimidal intermediate in the transition state. It is therefore probable that the bidentate coordination modes in the later transition states would require greater activation energy than for the monodentate ones. However, on the other hand the products of the latter case provide greater risk of reductive elimination, which have been largely circumvented by utilization of perfluorinated ligands in the study presented here.

In this paper, we describe the syntheses, structural characterization, and tunable emission properties of a series of neutral cycloaurated complexes of the type *cis*-[(N^C)AuL_n]

(17) Usón, R.; Vicente, J.; Cirac, J. A.; Chicote, M. T. *J. Organomet. Chem.* **1980**, *198*, 105–112.
(18) Vicente, J.; Chicote, M. T.; Arcas, A.; Artigao, M. *Inorg. Chim. Acta* **1982**, *65*, L251–L253.
(19) Vicente, J.; Chicote, M. T.; Arcas, A.; Artigao, M.; Jiménez, R. *J. Organomet. Chem.* **1983**, *247*, 123–129.
(20) Vicente, J.; Chicote, M. T.; Bermúdez, M. D.; Solans, X.; Font-Altaba, M. *J. Chem. Soc., Dalton Trans.* **1984**, 557–562.
(21) Vicente, J.; Chicote, M. T.; Cayuelas, J. A.; Fernandez-Baeza, J.; Jones, P. G.; Sheldrick, G. M.; Espinet, P. *J. Chem. Soc., Dalton Trans.* **1985**, 1163–1168.
(22) Vicente, J.; Chicote, M. T.; Bermúdez, M. D.; Sanchez-Santano, M. J.; Jones, P. G.; Fittschen, C.; Sheldrick, G. M. *J. Organomet. Chem.* **1986**, *310*, 401–409.
(23) Vicente, J.; Chicote, M. T.; Saura-Llamas, I.; Turpin, J.; Fernandez-Baeza, J. *J. Organomet. Chem.* **1987**, *333*, 129–137.
(24) Vicente, J.; Chicote, M. T.; Bermúdez, M. D.; Sanchez-Santano, M. J.; Jones, P. G. *J. Organomet. Chem.* **1988**, *354*, 381–390.
(25) Vicente, J.; Chicote, M. T.; Saura-Llamas, I.; Jones, P. G.; Meyer-Bäse, K.; Erdbrügger, C. F. *Organometallics* **1988**, *7*, 997–1006.
(26) Vicente, J.; Bermúdez, M. D.; Chicote, M. T.; Sanchez-Santano, M. J. *J. Chem. Soc., Chem. Commun.* **1989**, 141–142.
(27) Vicente, J.; Bermúdez, M. D.; Chicote, M. T.; Sanchez-Santano, M. J. *J. Organomet. Chem.* **1989**, *371*, 129–135.
(28) Vicente, J.; Bermúdez, M. D.; Chicote, M. T.; Sanchez-Santano, M. J. *J. Organomet. Chem.* **1990**, *381*, 285–292.
(29) Vicente, J.; Bermúdez, M. D.; Chicote, M. T.; Sanchez-Santano, M. J. *J. Chem. Soc., Dalton Trans.* **1990**, 1945–1950.
(30) Vicente, J.; Bermúdez, M. D.; Escribano, J.; Carrillo, M. P.; Jones, P. G. *J. Chem. Soc., Dalton Trans.* **1990**, 3083–3089.
(31) Vicente, J.; Bermúdez, M. D.; Sanchez-Santano, M. J.; Payá, J. *Inorg. Chim. Acta* **1990**, *174*, 53–56.
(32) Vicente, J.; Chicote, M. T.; Saura-Llamas, I. *J. Chem. Soc., Dalton Trans.* **1990**, 1941–1944.
(33) Vicente, J.; Chicote, M. T.; Lagunas, M. C.; Jones, P. G. *J. Chem. Soc., Dalton Trans.* **1991**, 2579–2583.
(34) Vicente, J.; Bermúdez, M. D.; Carrillo, M. P.; Jones, P. G. *J. Chem. Soc., Dalton Trans.* **1992**, 1975–1980.
(35) Vicente, J.; Bermúdez, M. D.; Carrillo, M. P.; Jones, P. G. *J. Organomet. Chem.* **1993**, *456*, 305–312.
(36) Vicente, J.; Bermúdez, M. D.; Carrión, F. J. *Inorg. Chim. Acta* **1994**, *220*, 1–3.
(37) Vicente, J.; Bermúdez, M. D.; Carrión, F. J.; Jones, P. G. *J. Organomet. Chem.* **1996**, *508*, 53–57.
(38) Vicente, J.; Chicote, M. T. *Coord. Chem. Rev.* **1999**, *195*, 1143–1161.
(39) Vicente, J.; Bermúdez, M. D.; Escribano, J. *Organometallics* **1991**, *10*, 3380–3384.
(40) Vicente, J.; Bermúdez, M. D.; Carrión, F. J.; Jones, P. G. *Chem. Ber.* **1996**, *129*, 1301–1306.
(41) Vicente, J.; Bermúdez, M. D.; Carrión, F. J.; Jones, P. G. *Chem. Ber.* **1996**, *129*, 1395–1399.
(42) Bardaji, M.; Laguna, A. *Inorg. Chim. Acta* **2001**, *318*, 38–44.
(43) Bardaji, M.; Laguna, A.; Vicente, J.; Jones, P. G. *Inorg. Chem.* **2001**, *40*, 2675–2681.
(44) Komiya, S.; Albright, T. A.; Hoffmann, R.; Kochi, J. K. *J. Am. Chem. Soc.* **1976**, *98*, 7255–7265.
(45) Cinellu, M. A.; Zucca, A.; Stoccoro, S.; Minghetti, G.; Manassero, M.; Sansoni, M. *J. Chem. Soc., Dalton Trans.* **1996**, 4217–4225.
(46) Kar, A.; Mangu, N.; Kaiser, H. M.; Beller, M.; Tse, M. K. *Chem. Commun.* **2008**, 386–388.
(47) Vicente, J.; Arcas, A.; Bautista, D.; Jones, P. G. *Organometallics* **1997**, *16*, 2127–2138.
(48) Vicente, J.; Abad, J. A.; Frankland, A. D.; de Arellano, M. C. R. *Chem.—Eur. J.* **1999**, *5*, 3066–3075.

Scheme 2

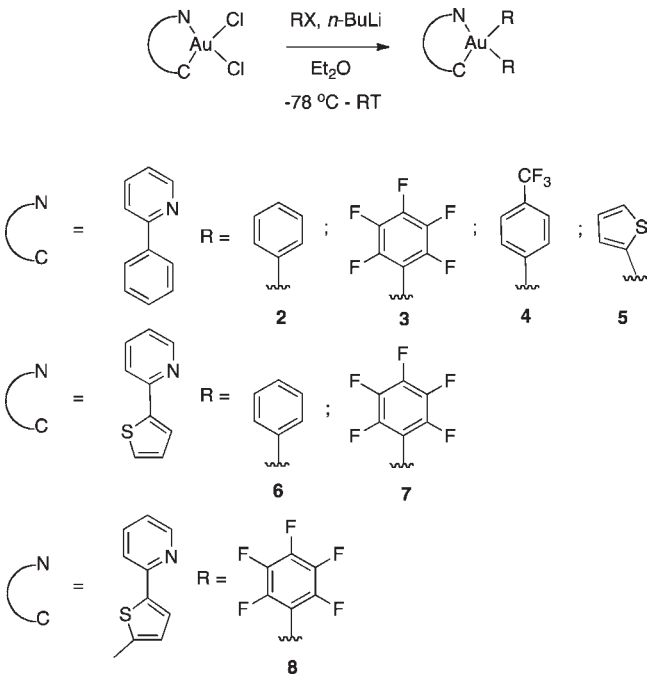

(L = aryl, n = 1, 2) most of which (**1**, **3**, **4**, **6**−**8**) exhibits good stability in common organic solvents and are also stable in the solid state for months under ambient conditions. Au(III) complexes, namely, *cis*-[(N^C)AuL] [N^C = 2-phenylpyridine (*ppy*), L = 1,1′-biphenyl (**1**)]; *cis*-[(N^C)-AuL_2] [N^C = 2-phenylpyridine, L = C_6H_5 (**2**), C_6F_5 (**3**), C_6H_4-CF_3-*p* (**4**), 2-C_4H_3S (**5**)]; [N^C = 2-(2-thienyl)-pyridine (*thpy*), L = C_6H_5 (**6**), C_6F_5 (**7**)]; [N^C = 2-(5-methyl-2-thienyl)pyridine (*5 m-thpy*), L = C_6F_5 (**8**)] were prepared from their corresponding cycloaurated Au(III) dichlorides (Scheme 2). Yields for complexes **2**−**8** were modest in the range 25−56% owing to the concomitant biaryl formation via reductive elimination as confirmed by ^{1}H NMR study. To our knowledge this is the first report of structurally characterized Au(III) monocyclometalated complexes with diaryl ligands. A cycloauration method described earlier in literature[49] was followed for obtaining dichloride precursor *cis*-[(N^C)$AuCl_2$] [N^C = 2-phenylpyridine (*ppy*)] for the synthesis of **1**−**5**. Complexes **6** and **7** were obtained from *cis*-[(N^C)$AuCl_2$] [N^C = 2-(2-thienyl)pyridine (*thpy*)] by following a procedure[50] which was also analogously adopted for synthesizing previously unknown *cis*-[(N^C)$AuCl_2$] [N^C = 2-(5-methyl-2-thienyl)pyridine (*5 m-thpy*)], the dihalide precursor for **8**. It is important to note that these starting materials do not exhibit RT phosphorescence.[51]

The stability of these complexes were found to depend significantly on the nature of the aryl ligands. Complexes containing nonperfluorinated groups showed signs of gradual decomposition in the solid state. The thermal stability of complexes **2** and **3** in solid state were studied using thermogravimetric analysis (TGA) (See Supporting Information, Figure S2). **2** and **3** showed initial weight loss ($\sim T_{10\%}$) in the interval 100−185 °C and 133−242 °C, respectively; the onset of total degradation (T_d) of **3** was observed at relatively higher temperature (T_d = 250 °C) than **2** (T_d = 180 °C).

Structural and Photophysical Characterization. X-ray single crystal structures were determined for all complexes except **3**. The perspective views of **1**, **2**, **5**, and **8** are shown in Figure 1 (for others see Figures S3−S5 in Supporting Information). As expected the Au(III) atom adopts a distorted square planar environment, the average Au−N bond distance is 2.102 Å and the mean Au−C_{aryl} bond distance of non-cyclometalated ligands (both *cis* and *trans* to nitrogen) was found to be 2.043 Å, values which correspond closely with those reported for similar [Au(C^N^C)] complexes[11,12] and the cationic diimine complexes.[9] The N−Au−C bite angles in **1**−**8** are restricted in the interval of 79.3−80.8° because of the steric requirements of the cyclometalating N^C ligands; consequently the respective *trans* angle to the ancillary carbons also deviates accordingly. The effect is more pronounced in **1** where there is an imposing steric congestion of both the *ppy* and biphenyl. Further, the molecular packing in the crystal structures of these complexes showed no Au···Au interactions; the shortest intermolecular Au···Au distance is 4.8022(1) Å in **1**. It is important to note that the crystal structures did not reveal the presence of any kind of solvent coordination to the metal center. Concentration dependent absorption studies of all the complexes in CH_2Cl_2 ($c \approx 10^{-6}$−10^{-4} mol dm^{-3}) did not change either the peak maxima or generate an additional low energy band confirming the absence of Au···Au interactions in solution and also precludes any excimeric (MMLCT) transitions.

Complexes **1**−**8** showed emission both in fluid solution at RT and in rigidified glass media (2-MeTHF) at 77 K. The spectroscopic data for complexes **1**−**8** are given in Table 1, and the absorption and emission profiles of complexes **1**−**3** and **6**−**8** are shown in Figure 2, respectively. Cyclometalated complexes with a *ppy* core exhibited intense absorption with lowest energy absorption maxima in the range λ = 316−338 nm. The *thpy* complexes **6** and **7** showed bathochromic shifts ($\lambda \sim 40$ nm) as expected for compounds, which inherently possess donor−acceptor (D-A) properties.[52] The red shift was more pronounced for the *5 m-thpy* complex **8** with the effect arising from the methyl substituent.[53] In general, the shape and position of absorption bands in electronic spectra resemble the skeletal vibrations of their respective ligands with a slight red shift (5−9 nm). This indicates that the π-conjugation is preserved through the metal site by mixing of the contributing frontier orbitals of the gold atom and the ligand.

Varying ligands ancillary to the cyclometalating (N^C) gold center had no marked effect on the absorption wavelengths. Increasing solvent polarity from toluene to tetrahydrofuran (THF) showed a slight hypsochromic shift ($\lambda \sim 6$ nm) for complexes **3**−**5** and for **7**−**8** indicating the ground state has more polar character as compared to the excited state. The emission spectra of the *ppy* complexes

(49) Constable, E. C.; Leese, T. A. *J. Organomet. Chem.* **1989**, *363*, 419–424.
(50) Fuchita, Y.; Ieda, H.; Wada, S.; Kameda, S.; Mikuriya, M. *J. Chem. Soc., Dalton Trans.* **1999**, 4431–4435.
(51) Mansour, M. A.; Lachicotte, R. J.; Gysling, H. J.; Eisenberg, R. *Inorg. Chem.* **1998**, *37*, 4625–4632.
(52) Tsuboyama, A.; Iwawaki, H.; Furugori, M.; Mukaide, T.; Kamatani, J.; Igawa, S.; Moriyama, T.; Miura, S.; Takiguchi, T.; Okada, S.; Hoshino, M.; Ueno, K. *J. Am. Chem. Soc.* **2003**, *125*, 12971–12979.
(53) Thomas, S. W., III; Venkatesan, K.; Müller, P.; Swager, T. M. *J. Am. Chem. Soc.* **2006**, *128*, 16641–16648.

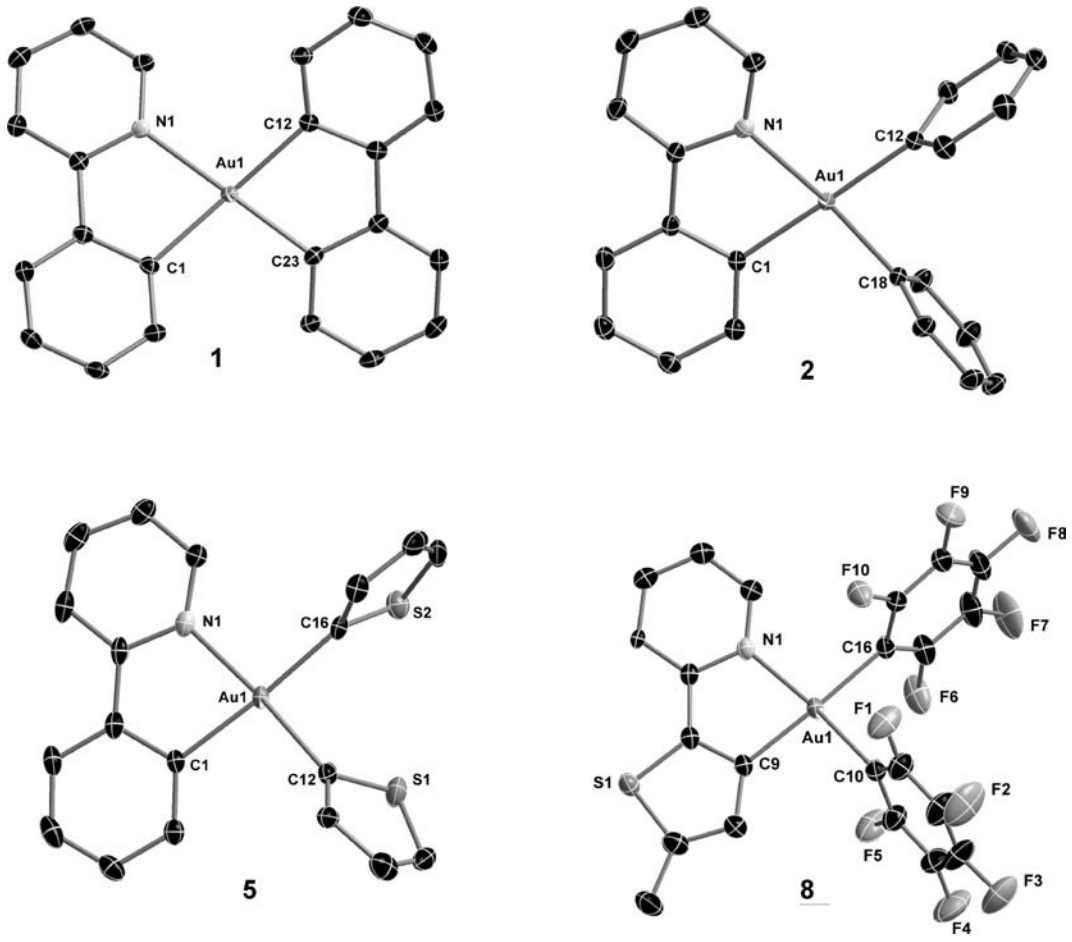

Figure 1. X-ray crystal structures of **1**, **2**, **5**, and **8** with selective atomic numbering scheme. Thermal ellipsoids are drawn at the 30% probability level. Hydrogen atoms and solvent molecules are omitted for clarity.

Table 1. Photophysical Properties of Complexes **1**−**8**

	room temperature solution (CH_2Cl_2)						
complex	absorption λ_{max}[nm] (ε_{max}/[dm^3 mol^{-1}cm^{-1}])	emission λ_{max}[nm]	τ [μs]	Φ_P[a]	k_r [s^{-1}] × 10^3	k_{nr} [s^{-1}] × 10^5	77 K glass[b] (2-MeTHF)
1	308 (5145), 317 (5385)	484, 506	1.10	3.7×10^{-3}	3.4	9.1	478, 513, 540
2	316 (8480)	467 (sh), 490, 519 (sh)	0.33	9.5×10^{-3}	28.7	30.0	453, 485, 512
3	324 (7214), 338 (5254, sh)	471 (sh), 493, 529 (sh)	4.41	1.0×10^{-3}	0.2	2.3	457, 489, 528
4	321 (8623)	470 (sh), 490, 522 (sh)	1.23	9.9×10^{-3}	8.0	8.1	452, 486, 517
5	319 (7884)	472 (sh), 492, 526 (sh)	0.53	1.9×10^{-2}	35.8	18.5	453, 489, 515
6	287 (13700), 357 (8070)	537, 569	1.15	2.5×10^{-3}	2.7	8.6	522, 541, 563
7	286 (12610), 363 (8540)	544, 577	1.12	1.5×10^{-3}	1.3	8.9	527, 545, 570
8	294 (8810), 380 (5760)	548, 592	1.21	2.0×10^{-3}	1.6	8.2	548, 593

[a] PL quantum yield determined with quinine sulfate as standard at 298 K. [b] Vibronic structured emission bands.

1−**5** in CH_2Cl_2 exhibit a low vibronic structured band with λ_{max} centered around 490 nm and more resolved progressive vibrational progression spacings of ∼1500 cm^{-1} at 77 K (2-MeTHF), which is close to stretching modes of C═C in pyridine systems. Again, the emission wavelengths did not change with different ancillary ligands like phenyl, pentafluorophenyl, *p*-trifluoromethylphenyl, and thienyl. Emission spectra of the *thpy* cyclometalates **6**−**8** depicted the same trend as for the *ppy* ones but systematically red-shifted in line with their respective absorption profiles. Vibrational spacings of about ∼1400 cm^{-1} were also observed here. On the basis of the above observations and considering the low radiative rate constant[54] $k_r \sim 10^3$−10^4 s^{-1} (see Table 1), the origin of the emission is assigned to intra-ligand charge transfer (^{3}ILCT) [π−π*] perturbed by the metal center. Stokes shifts of the lower lying emission in the range of 174−220 nm and lifetimes in the sub microsecond regime together with the observation of a 5 to 10-fold decrease in PL intensities upon exposure to molecular dioxygen suggest that the emission occurs from the triplet state. Isoelectronic biscyclometalated platinum(II) systems reported possess emission properties with more metal contribution in contrast to these Au(III)diaryl complexes.[55,56]

(54) Radiative (k_r) and non-radiative (k_{nr}) decay rates were estimated from the lifetime data (τ) using the formula $k_r = \Phi_P/\tau$ and $k_{nr} = (1 - \Phi_P)/\tau$ assuming radiative rate constants do not show significant temperature dependence from 77 to 298 K and k_{isc} is considered as unity.

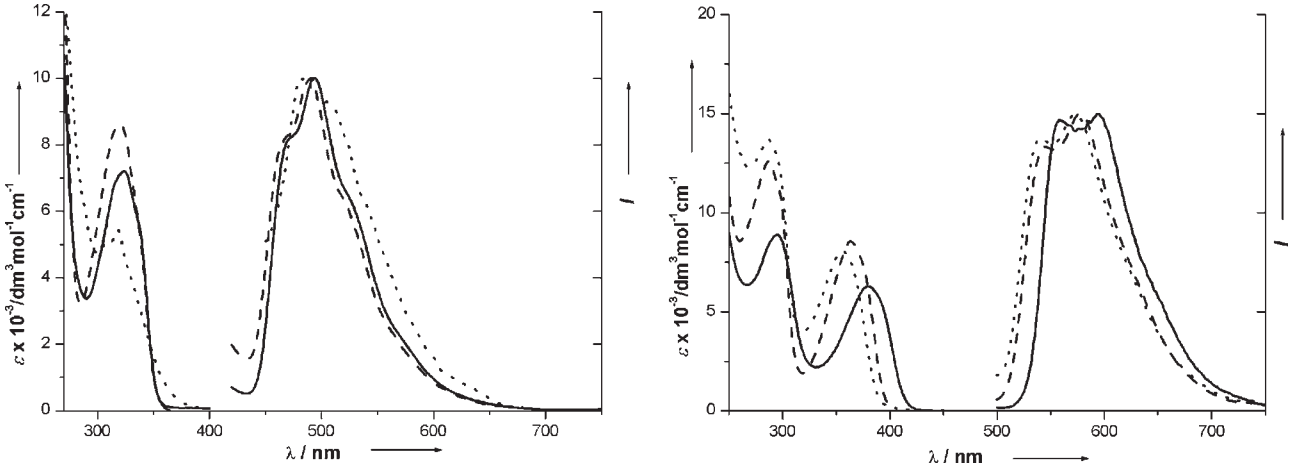

Figure 2. (left) Electronic absorption and normalized emission (*I*) spectra of **1** (dotted line), **2** (dashed line), **3** (solid line) in degassed CH_2Cl_2 at 298 K and (right) electronic absorption and normalized emission (*I*) spectra of **6** (dotted line), **7** (dashed line), **8** (solid line) in degassed CH_2Cl_2 at 298 K.

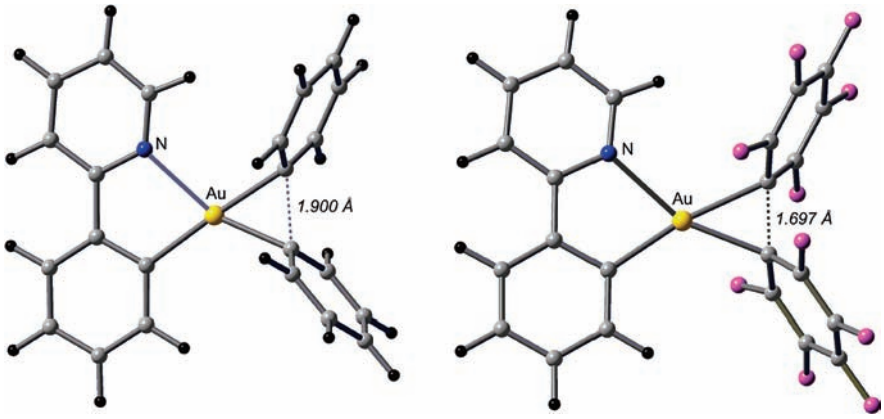

Figure 3. DFT optimized transition states **TS-2** (left) and **TS-3** (right).

DFT calculations. To gain insight into the properties of our Au(III) complexes, density functional theory (DFT) studies were carried out with the Gaussian03 program package[57] using the hybrid functional PBE1PBE[58] in conjunction with the Stuttgart/Dresden effective core potentials (SDD) basis set[59] for the Au center augmented with one f-polarization function ($\alpha = 1.050$) and the standard 6-31+G(d) basis set[60] for the remaining atoms. The relative stability of the compounds bearing different ancillary aryl ligands was first investigated. The transition states (**TS**) encountered during the intramolecular dimerization of C_6H_5 in **2** and C_6F_5 in **3** were successfully optimized and characterized (Figure 3). The $C_{aryl}\cdots C_{aryl}$ distance of 1.900 for **TS-2** and 1.697 Å for **TS-3** clearly indicates that the C−C bond formation in **2** occurs in an earlier stage in comparison with **3**. Furthermore, the electronic energies reveal decomposition barrier heights of 21.9 and 40.7 kcal/mol respectively and therefore confirm that the decomposition of the Au(III) complexes leading to the formation of corresponding biphenyl is significantly faster in **2**. This is also consistent with the experimental observation for these complexes.

Time-dependent density functional theory (TD-DFT)[61−63] combined with the conductive polarizable continuum model (CPCM)[64,65] was used to produce the ten lowest singlet−singlet and singlet−triplet vertical excitations calculated

(55) Chassot, L.; Muller, E.; von Zelewsky, A. *Inorg. Chem.* **1984**, *23*, 4249–4253.
(56) Chassot, L.; von Zelewsky, A. *Inorg. Chem.* **1987**, *26*, 2814–2818.
(57) Frisch, M. J.; Trucks, G. W.; Schlegel, H. B.; Scuseria, G. E.; Rob, M. A.; Cheeseman, J. R.; Montgomery Jr., J. A.; Vreven, T.; Kudin, K. N.; Burant, J. C.; Millam, J. M.; Iyengar, S. S.; Tomasi, J.; Barone, V.; Mennucci, B.; Cossi, M.; Scalmani, G.; Rega, N.; Petersson, G. A.; Nakatsuji, H.; Hada, M.; Ehara, M.; Toyota, K.; Fukuda, R.; Hasegawa, J.; Ishida, M.; Nakajima, T.; Honda, Y.; Kitao, O.; Nakai, H.; Klene, M.; Li, X.; Knox, J. E.; Hratchian, H. P.; Cross, J. B.; Bakken, V.; Adamo, C.; Jaramillo, J.; Gomperts, R.; Stratmann, R. E.; Yazyev, O.; Austin, A. J.; Cammi, R.; Pomelli, C.; Ochterski, J. W.; Ayala, P. Y.; Morokuma, K.; Voth, G. A.; Salvador, P.; Dannenberg, J. J.; Zakrzewski, V. G.; Dapprich, S.; Daniels, A. D.; Strain, M. C.; Farkas, O.; Malick, D. K.; Rabuck, A. D.; Raghavachari, K.; Foresman, J. B.; Ortiz, J. V.; Cui, Q.; Baboul, A. G.; Clifford, S.; Cioslowski, J.; Stefanov, B. B.; Liu, G.; Liashenko, A.; Piskorz, P.; Komaromi, I.; Martin, R. L.; Fox, D. J.; Keith, T.; Al-Laham, M. A.; Peng, C. Y.; Nanayakkara, A.; Challacombe, M.; Gill, P. M. W.; Johnson, B.; Chen, W.; Wong, M. W.; Gonzalez, C.; Pople, J. A. *Gaussian 03*; Gaussian, Inc.: Wallingford, CT, 2003.
(58) Adamo, C.; Barone, V. *J. Chem. Phys.* **1999**, *110*, 6158–6170.
(59) Dunning, T. H., Jr.; Hay, P. J. *Modern Theoretical Chemistry*; Plenum: New York, 1976; Vol. *3*.
(60) Ditchfie, R.; Hehre, W. J.; Pople, J. A. *J. Chem. Phys.* **1971**, *54*, 724–728.
(61) Stratmann, R. E.; Scuseria, G. E.; Frisch, M. J. *J. Chem. Phys.* **1998**, *109*, 8218–8224.
(62) Bauernschmitt, R.; Ahlrichs, R. *Chem. Phys. Lett.* **1996**, *256*, 454–464.
(63) Casida, M. E.; Jamorski, C.; Casida, K. C.; Salahub, D. R. *J. Chem. Phys.* **1998**, *108*, 4439–4449.
(64) Barone, V.; Cossi, M. *J. Phys. Chem. A* **1998**, *102*, 1995–2001.
(65) Cossi, M.; Rega, N.; Scalmani, G.; Barone, V. *J. Comput. Chem.* **2003**, *24*, 669–681.

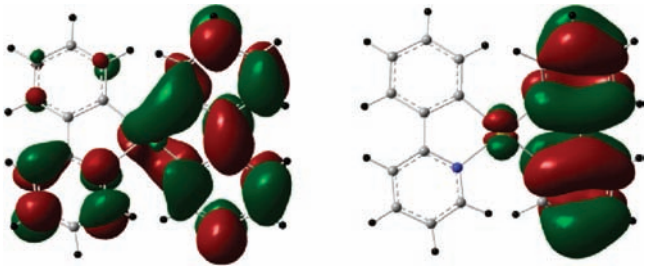

Figure 4. TD-DFT/CPCM calculated LUMO+2 (left) and HOMO (right) of the ground state geometry of **1**.

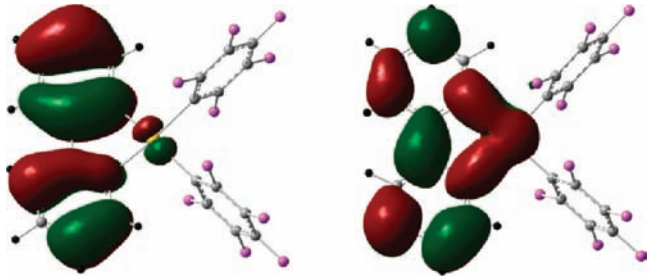

Figure 5. TD-DFT/CPCM calculated HOMO (left) and LUMO (right) of the ground state geometry of **3**.

at the ground state singlet S_0 optimized geometries. Despite the PBE1PBE[64] calculations having systematically provided underestimated absorption maxima λ_{max} by 17−20 nm (**5**−**8**) or 26−45 nm (**1**−**4**), the absorption properties of **1**−**8** and the trend observed in the experiments are well reproduced by the calculations (see Supporting Information, Table S5). For **2**−**8**, the lowest significant singlet transition $S_0 \rightarrow S_n$ (n = 1 for **3**, **6**, **7**, **8**; n = 2 for **2**, **4**; n = 3 for **5**) is the one showing the largest coefficient of the calculated excited states. The frontier molecular orbitals involved in the dominant excitation are almost exclusively located on the N^C ligands, *ppy* for **2**−**5** or *thpy* for **6**−**8** as expected. This can be attributed to a transition with an intraligand charge transfer ^{1}ILCT [$\pi \rightarrow \pi^*$] character. For **1**, the picture is different since three low energy transitions of similar intensity at 311, 288, and 282 nm were calculated. The two lowest-lying transitions $S_0 \rightarrow S_3$ and $S_0 \rightarrow S_6$ at 311 and 288 nm are due to the one-electron excitations from HOMO-2→LUMO and HOMO-4→LUMO, respectively (hereafter H = HOMO, L = LUMO). H-2 and H-4 are mainly composed of π orbitals of biphenyl (*bip*) and *ppy*, whereas L is dominantly localized on *ppy* (86%), consequently the corresponding band can be attributed to a transition with an admixture of ligand-to-ligand ^{1}LLCT [π(*bip*)→π^*(*ppy*)] and intraligand ^{1}ILCT [$\pi \rightarrow \pi^*$ (*ppy*)] characters. The $S_0 \rightarrow S_8$ transition at 282 nm with the most relevant contribution from H→L+3 accounts for an inverse charge transfer since H is at 97% on *bip* and L+3 is totally delocalized over the whole molecule.

The lowest vertical triplet S_0-T_1 transition of **1** is $\pi-\pi^*$ type defined by the configuration H→L+2 where H is mainly a π orbital localized at the *bip* ligand (97%) and L+2 is a π^* orbital delocalized at 75% on the *bip*, 17% on the *ppy* ligand, and at 8% on the metal center (Figure 4). This indicates that the excited state contains both ^{3}LLCT [π(*bip*)→π^*(*ppy*)] and ^{3}ILCT [π(*bip*)→π^*(*bip*)] characters. The DFT optimized triplet state is in agreement with the lowest-lying $\pi-\pi^*$ transition since the main variations of the geometrical parameters relative to the ground state of **1** correspond well to the electronic transition from H to L+2, especially for the C−C bond bridging the two rings of the *bip*, the bond distance of which is hardly shortened by 0.081 Å in the triplet state, a consequence of the π antibonding character of the C−C bond in H and π bonding in L+2 (which became the lower- and higher-energy singly occupied molecular orbital of the optimized triplet state). All bond distances around the metal center are also slightly shortened in the triplet state. The emission maximum of **1** was estimated by the solvent-corrected (CH_2Cl_2) energy difference between the optimized ground and triplet states. The calculated λ_{max} of 486 nm is in good agreement with the experimental data of 506 nm. In the other *ppy*-containing compounds **2**−**5**, the optimized triplet states also correspond very well to the lowest vertical singlet−triplet transitions S_0-T_1. The main difference in comparison with **1** is that the orbitals involved in the $\pi-\pi^*$ transition are mainly located on the *ppy* ligand: H-1→L (83→94%), H→L (98→92%), H-1→L (92→95%), H-2→L (95→95%) for **2**−**5**, respectively. This indicates that the excited state exhibits a ^{3}ILCT [$\pi \rightarrow \pi^*$ (*ppy*)] character, only slightly perturbed by the metal center (2−6%) (Figure 5). As a result, it was found that the main geometric changes appear in the *ppy* group where the bond distance of the C−C linker is shortened by 0.078−0.079 Å compared to the ground state parameters. The estimated emission maxima based on the calculated ground and triplet state energies correlate successfully with the experimental emission wavelengths (in parentheses) with 466 (490), 472 (493), 468 (490), and 470 (492) nm for **2**−**5**, respectively.

The same study was adopted for the *thpy* species **6**−**8**. For all the three compounds, the lowest vertical triplet S_0-T_1 transition corresponds to the H→L excitation. H and L orbitals are at 96−99% and 92−93% located on the *thpy* ligand respectively, indicating a ^{3}ILCT [$\pi \rightarrow \pi^*$ (*thpy*)] character of the triplet state. The main variations in the geometry of the optimized triplet states are no longer observed on the C−C bridge (only −0.049 to −0.056 Å) but rather in the five-membered thienyl ring with significant elongations of four over five bond distances (+0.011 to +0.096 Å), in agreement with the shape of the π/π^* H and L orbitals. The significant red-shifted emission of **6**−**8** in comparison with **1**−**5** is also well reproduced by our calculations with 569 (569), 572 (577), and 604 (592) nm for **6**−**8**, respectively.

Conclusion

We have shown for the first time that cyclometalated compounds of the type *cis*-[(N^C)AuL$_n$] (L = aryl, n = 2) are stable with the incorporation of fluorinated functional groups on the aryl rings. They show phosphorescence emission at RT in fluid solution and their emission wavelengths can be tuned by changing the cyclometalating ligand. DFT calculations in conjunction with experimental work have ascertained the relative stability of the complexes and the nature of the triplet excited state. The stability and ease of tunability demonstrated in this work make these systems amenable for the development of efficient neutral triplet phosphors for OLED applications. Several strategies are currently being pursued in

our group for the improvement of quantum yields and to obtain blue triplet emitters based on these Au(III) complexes.

Experimental Section

Materials and General Methods. Commercially available reagents were purchased from Aldrich and were used as such without further purification. Diethylether used in reactions was dried by distillation under N_2 atmosphere using sodium benzophenone ketyl radical prior to use. Sodium tetrachloroaurate (III) dihydrate was purchased from Strem chemicals. Gold(III) dichloride precursor complex [(N^C)$AuCl_2$][N^C = 2-phenylpyridine (*ppy*)] (**A**) was prepared according to a known procedure[49] and [(N^C)$AuCl_2$][N^C = 2-(2-thienyl)pyridine (*thpy*)] (**B**) was synthesized based on a different cycloauration procedure.[50] A procedure analogous to the latter was adopted for preparing precursor complex [N^C = 2-(5-methyl-2-thienyl)pyridine (*5 m-thpy*)][$AuCl_2$] (**C**), which is described below. All manipulations requiring an inert atmosphere were carried out using standard Schlenk techniques under dinitrogen. ^{1}H, ^{13}C{^{1}H}, and ^{19}F NMR spectra were recorded on Bruker AV2−400 (400 MHz) or AV-500 (500 MHz) spectrometers. Chemical shifts (δ) are reported in parts per million (ppm) referenced to tetramethylsilane (δ 0.00 ppm) using the residual proton solvent peaks as internal standards (^{1}H NMR experiments) or the characteristic resonances of the solvent nuclei (^{13}C NMR experiments). ^{19}F NMR was referenced to $CFCl_3$ (δ 0.00 ppm). Coupling constants (J) are quoted in hertz (Hz), and the following abbreviations are used to describe the signal multiplicities: s (singlet); d (doublet); t (triplet); q (quartet); m (multiplet); dd (doublet of doublet); td (triplet of doublet); dm (doublet of multiplet). Proton and carbon assignments have been made using routine one and two-dimensional NMR spectroscopies where appropriate. Infrared (IR) spectra were recorded on a Perkin-Elmer 1600 Fourier Transform spectrophotometer using KBr pellet with frequencies (ν_{max}) quoted in wavenumbers (cm^{-1}). Elemental microanalysis was carried out with Leco CHNS-932 analyzer. Mass spectra were run on a Finnigan-MAT-8400 mass spectrometer. TLC analysis was performed on precoated Merck Silica Gel 60F_{254} slides and visualized by luminescence quenching either at (short wavelength) 254 nm or (long wavelength) 365 nm. Chromatographic purification of products was performed on a short column (length 15.0 cm: diameter 1.5 cm) using silica gel 60, 230−400 mesh using a forced flow of eluent. UV−vis measurements were carried out on a Perkin-Elmer Lambda 19 UV/vis spectrophotometer. Emission spectra were acquired on Perkin-Elmer spectrophotometer using 450 W xenon lamp excitation by exciting at the longest-wavelength absorption maxima. All samples for emission spectra were degassed by at least three freeze−pump−thaw cycles in an anaerobic cuvette and were pressurized with N_2 following each cycle. 77 K emission spectra were acquired in frozen 2-methyltetrahydrofuran (2-MeTHF) glass. Luminescence quantum yields of (ϕ) were determined at 298 K (estimated uncertainty ±15%) using standard methods;[66] wavelength-integrated intensities (I) of the corrected emission spectra were compared to iso-absorptive spectra of quinine sulfate standard (ϕ_r = 0.54 in 1N H_2SO_4 air-equilibrated solution) and were corrected for solvent refractive index. Phosphorescence lifetime measurements were performed on an Edinburgh FLS920 spectrophotometer, using nF900 with 30000 Hz frequency, with 15 nm excitation and 15 nm emission slit widths. Thermogravimetric analysis (TGA) was done using a NETZSCH STA 449C instrument. The thermal stability of the samples under a nitrogen atmosphere was determined by measuring their weight loss while heating at a rate of 1 °C min^{-1} from 25 to 600 °C.

Computational Details. All calculations were performed with the Gaussian 03 program package[57] using the hybrid functional PBE1PBE[58] in conjunction with the Stuttgart/Dresden effective core potentials (SDD) basis set[59] for the Au center augmented with one f-polarization function (exponent α = 1.050) and the standard 6-31+G(d) basis set[60] for the remaining atoms. Several exchange-correlation functionals (B3LYP,[67−69] MPW1K,[70,71] BB1K,[67,72,73] PBE1PBE,[58] G96LYP,[68,72] TPSS[74,75] and TPSSLYP1W[75]) were tested on the geometry structures of **1** and **2**; the hybrid PBE1PBE provided the best match with the geometrical X-ray data and was selected for our study (see Supporting Information). Full geometry optimizations without symmetry constraints were carried out in the gas phase for both the singlet ground states (S_0) and the lowest triplet excited states (T_1). The optimized geometries were confirmed to be potential energy minima by vibrational frequency calculations at the same level of theory, as no imaginary frequencies were found. The first 10 singlet−singlet and singlet−triplet transition energies were computed at the optimized S_0 geometries, by using the time-dependent DFT (TDDFT) methodology.[61−63] Solvent effects were taken into account using the conductive polarizable continuum model (CPCM)[64,65] with dichloromethane as solvent for single-point calculations on all optimized gas-phase geometries.

X-ray Diffraction Analyses. Relevant details about the structure refinements are given in Supporting Information, Tables S1 and S2, and selected geometrical parameters are included in the captions of the corresponding figures (Supporting Information, Figures S3, S4, and S5). Intensity data were collected at 183(2) K an Oxford Xcalibur diffractometer (4-circle kappa platform, Ruby CCD detector, and a single wavelength Enhance X-ray source with Mo K_α radiation, λ = 0.71073 Å)[76] The selected suitable single crystals were mounted using polybutene oil on the top of a glass fiber fixed on a goniometer head and immediately transferred to the diffractometer. Pre-experiment, data collection, data reduction, and analytical absorption corrections[77] were performed with the Oxford program suite CrysAlisPro.[78] The crystal structures were solved with SHELXS-97[79] using direct methods. The structure refinements were performed by full-matrix least-squares on F^2 with SHELXL-97.[79] All programs used during the crystal structure determination process are included in the WINGX software.[80] The program PLATON[81] was used to check the result of the X-ray analyses. CCDC-778147−778153 contain the supplementary crystallographic data (excluding structure factors) for this paper. These data can be obtained free of charge from The Cambridge Crystallographic Data Center via www.ccdc.cam.ac.uk/data_request/cif.

[N^C = 2-(5-Methyl-2-thienyl)pyridine][$AuCl_3$]. 2-(5-methyl-2-thienyl)pyridine (0.150 g, 0.856 mmol) in acetonitrile (3.5 mL) was added to Na[$AuCl_4$]·2H_2O (0.313 g, 0.787 mmol) in H_2O (3.5 mL), and the resulting mixture was stirred at room temperature for 12 h. The orange solids that precipitated out were

(66) Demas, J. N.; Crosby, G. A. *J. Phys. Chem.* **1971**, *75*, 991–1024.

(67) Becke, A. D. *Phys. Rev. A* **1988**, *38*, 3098–3100.
(68) Lee, C. T.; Yang, W. T.; Parr, R. G. *Phys. Rev. B* **1988**, *37*, 785–789.
(69) Stephens, P. J.; Devlin, F. J.; Chabalowski, C. F.; Frisch, M. J. *J. Phys. Chem.* **1994**, *98*, 11623–11627.
(70) Lynch, B. J.; Fast, P. L.; Harris, M.; Truhlar, D. G. *J. Phys. Chem. A* **2000**, *104*, 4811–4815.
(71) Lynch, B. J.; Zhao, Y.; Truhlar, D. G. *J. Phys. Chem. A* **2003**, *107*, 1384–1388.
(72) Gill, P. M. W. *Mol. Phys.* **1996**, *89*, 433–445.
(73) Zhao, Y.; Lynch, B. J.; Truhlar, D. G. *J. Phys. Chem. A* **2004**, *108*, 2715–2719.
(74) Tao, J. M.; Perdew, J. P.; Staroverov, V. N.; Scuseria, G. E. *Phys. Rev. Lett.* **2003**, *91*, 146401.
(75) Dahlke, E. E.; Truhlar, D. G. *J. Phys. Chem. B* **2005**, *109*, 15677–15683.
(76) *Xcalibur CCD System*; Oxford Diffraction Ltd: Abingdon, Oxfordshire, England, 2007.
(77) Clark, R. C.; Reid, J. S. *Acta Crystallogr., Sect. A* **1995**, *51*, 887–897.
(78) *CrysAlisPro*, Versions 1.171.32.34d-55; Oxford Diffraction Ltd: Abingdon, Oxfordshire, England.
(79) Sheldrick, G. M. *Acta Crystallogr., Sect. A* **2008**, *64*, 112–122.
(80) Farrugia, L. J. *J. Appl. Crystallogr.* **1999**, *32*, 837.
(81) Spek, A. L. *J. Appl. Crystallogr.* **2003**, *36*, 7–13.

filtered off, and the precipitate was successively washed with water and diethylether to give the title product. Yield = 0.278 g, 68%. Positive EI-MS: m/z: 476 $[M]^+$; IR (KBr): ν(Au−Cl) 363 cm^{-1}; ^1H NMR (500 MHz, CD_3CN, 298 K) δ 2.63 (s, 3H), 7.06 (d, J = 4.0 Hz, 1H), 7.72 (t, J = 5.5 Hz, 1H), 7.76 (d, J = 4.0 Hz, 1H), 7.79 (d, J = 6.5 Hz, 1H), 8.22 (t, J = 5.5 Hz, 1H), 8.93 (d, J = 6.0 Hz, 1H); ^{13}C NMR (125 MHz, CD_3CN, 298 K) δ 15.2, 127.2, 128.0, 130.4, 132.6, 136.2, 143.4, 147.6, 150.9, 153.4; elemental analysis (%) calcd for $C_{10}H_9AuCl_3NS$: C, 25.10; H, 1.90; N, 2.93. Found: C, 25.00; H, 1.88; N, 2.99.

[N^C = 2-(5-Methyl-2-thienyl)pyridine][$AuCl_2$] (C). Silver(I) tetrafluoroborate (0.084 g, 0.431 mmol) was added to [N^C = 2-(5-methyl-2-thienyl)pyridine][$AuCl_3$] (0.200 g, 0.418 mmol) in dichloromethane (60 mL), and the resulting mixture was refluxed for 4 h. After filtration under hot condition, the filtrate was evaporated to dryness, and the residue was washed with a minimum amount of acetonitrile (3.0 mL) to remove silver salts, giving the title complex **C** as a green solid. Yield = 0.073 g, 40%. Positive EI-MS: m/z: 405 $[M - Cl]^+$; IR (KBr): ν (Au−Cl) 304, 354 cm^{-1}; ^1H NMR (500 MHz, DMSO-d_6, 298 K): δ 2.60 (s, 3H), 7.07 (s, 1H), 7.56 (td, J = 6.0, 1.5 Hz, 1H), 7.86 (d, J = 7.5 Hz, 1H), 8.25 (td, J = 6.0, 1.5 Hz, 1H), 9.25 (d, J = 5.5 Hz, 1H); ^{13}C NMR (125 MHz, DMSO-d_6, 298 K): δ 15.6, 120.3, 122.4, 126.0, 137.0, 144.0, 144.2, 147.8, 150.3, 158.3; elemental analysis (%) calcd for $C_{10}H_8AuCl_2NS$; C, 27.17; H, 1.82; N, 3.17 Found: C, 27.32; H, 1.94; N, 3.19.

***cis*-[(N^C)AuL][N^C = 2-phenylpyridine, L = 2,2′-biphenyl] (1).** To 2,2′-Dibromobiphenyl (88.0 mg, 0.28 mmol) in dry diethylether (5.0 mL), n-BuLi (0.35 mL, 0.55 mmol, 1.6 M in hexanes) was added slowly via syringe at −78 °C and then stirred for 1 h at RT. The dilithiated solution was then transferred into a flask containing diethylether suspension of **A** (100.0 mg, 0.23 mmol) and AgOTf (4.6 mg, 0.018 mmol) maintained at −78 °C. The cold bath was removed immediately after addition, and the mixture was allowed to stir for 10 h. It was then quenched by addition of water (5.0 mL) and extracted with dichloromethane (2 × 15 mL). The separated organic layers were combined and dried over $MgSO_4$. Filtration followed by concentration of the solvent in vacuo gave the crude product as a light brown solid. It was washed with pentane (5.0 mL), and the residue was purified by flash column chromatography using silica gel (eluent: Hexane/EtOAc = 3/2) to afford **1** as an off-white solid. Single crystals suitable for X-ray diffraction analysis were obtained from slow evaporation by layering of pentane over concentrated solution of the complex in dichloromethane at 0−5 °C. Yield = 15.0 mg, 12%. IR: (KBr) ν_{max} 3414, 2924, 2853, 1638, 1618, 1605, 1581, 1482, 1429, 1160, 1104, 1013, 736, 734, 726, 615, 479 cm^{-1}; ^1H NMR (500 MHz, CD_2Cl_2, 298 K): δ 7.11 (td, J = 6.0, 1.0 Hz, 1H), 7.18−7.25 (m, 3H), 7.36 (td, J = 6.5, 1.0 Hz, 1H), 7.50−7.57 (m, 4H), 7.62 (d, J = 6.5 Hz, 1H), 7.92 (d, J = 8.5 Hz, 1H), 7.95 (d, J = 8.5 Hz, 1H), 8.08 (d, J = 6.5 Hz, 2H), 8.19 (d, J = 7.0 Hz, 1H), 9.2 (d, J = 5.5 Hz, 1H); $^{13}C\{^1H\}$ NMR (125 MHz, CD_2Cl_2, 298 K): δ 121.1, 121.3, 121.7, 123.8, 125.0, 126.5, 126.9, 127.0, 127.1, 127.5, 131.1, 132.0, 134.0, 135.7, 140.7, 147.3, 148.5, 149.4, 154.0, 155.8, 167.3, 171.4, 174.1; elemental analysis (%) calcd for $C_{23}H_{16}AuN$; C, 54.88; H, 3.20; N, 2.78; Found: C, 54.60; H, 3.12; N, 2.68 (Note: ^1H NMR and IR analyses of late eluting fractions from the column (eluent:ethyl acetate) suggest the presence of about 10% of monocoordinated biphenyl Au(III) chloride complex, characterization details of which are not presented here).

General Procedure for the Synthesis of Cyclometalated Au (III) Complexes (2−8). n-BuLi (0.52 mmol, 1.6 M in hexanes) was added via syringe to a cooled (−78 °C) solution of the aryl halide (0.50 mmol) in dry diethylether under nitrogen atmosphere and stirred for 20 min at that temperature. It was then transferred via cannula into a flask containing an diethylether suspension of cycloaurated Au(III)dichloride (0.22 mmol) precooled at −78 °C. This temperature was maintained for 20 min and then the mixture was allowed to warm to RT and stirred further for 1 h. (Note: At this stage the reaction mixture turns dark (violet coloration), more in the case of non-fluorinated analogues indicating partial decomposition of the product to metallic gold). TLC examination (EtOAc/Hexane = 1/5) of the reaction mixture at this stage usually showed two major spots, the first ($R_f \sim 0.7$) corresponding to the homocoupled diaryl and the second being the desired organometallic product ($R_f \sim 0.4$) which also gets faintly illuminated in UV lamp longwave (365 nm). The reaction was quenched by addition of water (5 mL) followed by extraction with ethyl acetate/dichloromethane. After separation, the organic layer was dried over $MgSO_4$ and concentrated in vacuo to obtain the crude product. Purification on a short silica gel column (eluent: EtOAc and hexane mixture) was adopted to obtain analytically pure products. Some derivatives were prepared with modifications in the general procedure and are described individually.

***cis*-[(N^C)AuL_2][N^C = 2-phenylpyridine, L = C_6H_5] (2).** Phenyllithium (0.61 mL, 0.746 mmol, 1.8 M soln. in di-n-butylether) was syringed into a Schlenk flask containing cooled (−78 °C) suspension of **A** (150.0 mg, 0.35 mmol) in diethylether (5.0 mL) under N_2 atmosphere. The cold bath was removed 15 min after addition, and the reaction mixture was allowed to warm up to RT and stirred for 12 h. The reaction was then quenched by adding H_2O (8.0 mL) and extracted with dichloromethane (2 × 10 mL). The combined dichloromethane layers were dried over $MgSO_4$, filtered, and concentrated in vacuo to yield the crude product. Further purification by flash column chromatography using silica gel (eluent: Hexane/EtOAc = 3/1) afforded **2** as off-white solid. Single crystals suitable for X-ray diffraction analysis were obtained from slow evaporation by layering of pentane over concentrated solution of the complex in dichloromethane at 0−5 °C. Yield = 100.0 mg, 55.0%. IR (KBr): ν_{max} 3413, 2924, 2853, 1638, 1618, 1605, 1571, 1478, 1422, 1163, 1062, 1019, 751, 734, 695, 631, 471 cm^{-1}; ^1H NMR (500 MHz, $CDCl_3$, 298 K): δ 7.03−7.09 (m, 3H), 7.15 (t, J = 8.0 Hz, 2H), 7.19 (t, J = 7.0 Hz, 1H), 7.22−7.31 (m, 4H), 7.45 (d, J = 8.0 Hz, 2H), 7.49 (d, J = 7.0 Hz, 2H), 7.80 (d, J = 7.5 Hz, 1H), 7.92−7.98 (m, 2H), 8.18 (d, J = 5 Hz, 1H); $^{13}C\{^1H\}$NMR (125 MHz, $CDCl_3$, 298 K): δ 119.9, 123.1, 124.1, 124.6, 126.2, 127.1, 127.2, 128.7, 131.1, 132.4, 135.2, 135.9, 140.1, 142.0, 145.8, 149.2, 166.7, 166.9, 169.6; elemental analysis (%) calcd for $C_{23}H_{18}AuN$; C, 54.66; H, 3.59; N, 2.77; Found: C, 54.52; H, 3.42; N, 2.80.

***cis*-[(N^C)AuL_2][N^C = 2-phenylpyridine, L = C_6F_5] (3).** This reaction was performed according to the general procedure. To iodopentafluorobenzene (153.2 mg, 0.521 mmol) in diethylether (5.0 mL), n-BuLi (0.33 mL, 0.541 mmol, 1.6 M soln. in hexanes) was added. The lithiated product was transferred to a flask containing **A** (100.0 mg, 0.237 mmol) in diethylether. The crude product thus obtained after workup was purified by flash column chromatography using silica gel (eluent: Hexane/EtOAc = 5/1) to obtain an off-white solid. The solid was further recrystallized from a mixture of ether and pentane to obtain **3** as a white solid. Yield = 66 mg, 40%. IR (KBr): ν_{max} 3414, 2923, 2853, 1738, 1637, 1610, 1509, 1462, 1477, 1365, 1309, 1263, 1073, 967, 906, 885, 812, 785, 757, 732, 629, 466 cm^{-1}; ^1H NMR (500 MHz, $CDCl_3$, 298 K): δ 6.83 (d, J = 7.5 Hz, 1H), 7.29 (td, J = 6.5, 1.5 Hz, 1H), 7.37 (t, J = 7.0 Hz, 2H), 7.78 (d, J = 7.5 Hz, 1H), 8.04 (d, J = 8.0 Hz, 1H), 8.12 (td, J = 8.0, 1.5 Hz, 1H), 8.25 (d, J = 8.0 Hz, 1H); $^{13}C\{^1H\}$ NMR (125 MHz, $CDCl_3$, 298 K): δ 120.8, 124.3, 125.2, 127.8, 132.3, 133.8, 137.5 (dm, $^1J_{C-F}$ = 251.0 Hz), 138.1 (dm, $^1J_{C-F}$ = 251.0 Hz), 139.5 (dm, $^1J_{C-F}$ = 251.0 Hz), 141.8, 144.1 (dm, $^1J_{C-F}$ = 232.0 Hz), 145.1, 146.5 (dm, $^1J_{C-F}$ = 232.0 Hz), 149.3, 158.0, 165.8, 166.7, (note: resonances for 2C submerged in baseline); ^{19}F NMR (470 MHz, $CDCl_3$, 298 K): δ −122.2 (m, 2F, o-C_6F_5), −122.3 (m, 2F, o-C_6F_5), −157.8 (t, J = 20.2 Hz, 1F, p-C_6F_5), −158.7 (t, J = 20.2 Hz, 1F, p-C_6F_5), −161.5 (t, J = 19.2 Hz, 2F, m-C_6F_5), −162.5

(t, J = 19.7 Hz, 2F, *m*-C_6F_5); elemental analysis (%) calcd. for: $C_{23}H_8AuF_{10}N \cdot CH_3C(O)OC_2H_5$: C, 41.93; H, 2.09; N, 1.81; Found: C, 41.86; H, 2.00; N, 1.97.

***cis*-[(N^C)AuL$_2$][N^C = 2-phenylpyridine, L = C_6H_4-CF_3-*p*] (4).** This reaction was performed according to the general procedure. To 1-bromo-4-(trifluoromethyl)benzene (117.2 mg, 0.521 mmol) in diethylether (5.0 mL), *n*-BuLi (0.33 mL, 0.541 mmol, 1.6 M soln. in hexanes) was added. The lithiated product was then transferred to a flask containing **A** (100.0 mg, 0.237 mmol) in diethylether. The crude product thus obtained after workup was purified by flash column chromatography using silica gel (eluent: Hexane/EtOAc = 5/1) to obtain **4** as off-white solid. Single crystals suitable for X-ray diffraction analysis were obtained from slow evaporation by layering of pentane over concentrated solution of the complex in dichloromethane at 0−5 °C. Yield = 51.0 mg, 33%. IR (KBr): ν_{max} 3413, 3064, 1637, 1607, 1482, 1439, 1390, 1327, 1157, 1120, 1087, 1078, 1066, 1050, 1013, 906, 820, 755, 733, 679, 666, 648, 599, 478 cm^{-1}; ^{1}H NMR (500 MHz, CD_2Cl_2, 298 K): δ 6.89 (dd, J = 8.5, 1.5 Hz, 1H), 7.23−7.30 (m, 3H), 7.41 (d, J = 8.5 Hz, 2H), 7.48 (d, J = 8 Hz, 2H), 7.60 (d, J = 9.0 Hz, 2H), 7.66 (d, J = 8.5 Hz, 2H), 7.82 (dd, J = 8.5, 1.5 Hz, 1H), 7.99−8.03 (m, 2H), 8.05 (d, J = 8.0 Hz, 1H); ^{13}C{^{1}H} NMR (125 MHz, CD_2Cl_2, 298 K): δ 120.7, 121.9, 123.9, 124.0, 124.8, 125.2, 125.3 (q, $^2J_{C-F}$ = 3.8 Hz), 125.6 (q, $^2J_{C-F}$ = 3.9 Hz), 126.5 (q, $^1J_{C-F}$ = 32.0 Hz), 127.2 (q, $^1J_{C-F}$ = 31.6 Hz), 131.5, 133.0, 135.7, 135.8, 141.3, 146.2, 147.0, 149.5, 167.0, 167.1, 172.4; ^{19}F NMR (376 MHz, $CDCl_3$, 298 K): δ −62.19 (s, 3H), −62.22 (s, 3H); elemental analysis (%) calcd for: $C_{25}H_{16}AuF_6N$: C, 46.82; H, 2.51; N, 2.18 Found: C, 46.70; H, 2.65; N, 2.18.

***cis*-[(N^C)AuL$_2$][N^C = 2-phenylpyridine, L = C_4H_3S] (5).** This reaction was performed according to the general procedure. To 2-bromothiophene (0.83 mL, 0.52 mmol) in diethylether (5.0 mL), *n*-BuLi (0.33 mL, 0.541 mmol, 1.6 M soln. in hexanes) was added, and this mixture was transferred to flask containing **A** (100.0 mg, 0.237 mmol) in diethylether. The crude product thus obtained after workup was purified by column chromatography on silica gel (eluent: Hexane/EtOAc = 5/1) to obtain **5** as off-white solid. Single crystals suitable for X-ray diffraction analysis were obtained from slow evaporation by layering of pentane over concentrated solution of the complex in dichloromethane at 0−5 °C. Yield = 68 mg, 55%. IR (KBr): ν_{max} 3413, 1638, 1617, 1481, 1437, 1402, 1259, 1202, 1064, 1028, 834, 806, 751, 690, 626, 471 cm^{-1}; ^{1}H NMR (500 MHz, $CDCl_3$, 298 K): δ 6.98 (d, J = 5.0 Hz, 1H), 7.04 (d, J = 5.0 Hz, 1H), 7.12−7.14 (m, 1H), 7.16−7.18 (m, 1H), 7.24−7.28 (m, 2H), 7.29−7.32 (m, 2H), 7.47 (d, J = 5.0 Hz, 1H), 7.61 (d, J = 5.0 Hz, 1H), 7.75−7.77 (m, 1H), 7.95−8.00 (m, 2H), 8.35 (d, J = 5.0 Hz, 1H); ^{13}C{H} NMR (125 MHz, $CDCl_3$, 298 K): δ 119.9, 123.4, 124.3, 125.0, 125.6, 127.9, 129.4, 131.5, 132.3, 135.3, 140.8, 145.5, 149.4, 151.7, 158.7, 160.3, 163.2, 164.7, 166.8; elemental analysis (%) calcd for $C_{19}H_{14}AuNS_2$: C, 44.10; H, 2.73; N, 2.71; Found: C, 43.90; H, 2.87; N, 2.63.

***cis*-[(N^C)AuL$_2$] [N^C = 2-(2-thienyl)pyridine, L = C_6H_5] (6).** Phenyllithium (0.64 mL, 0.780 mmol, 1.8 M soln. in di-*n*-butyl ether) was slowly syringed into a Schlenk flask containing cooled (−78 °C) suspension of **B** (100.0 mg, 0.233 mmol) in diethylether (5.0 mL) under N_2 atmosphere. The cold bath was removed after 15 min, and the reaction mixture was allowed to warm up to RT and stirred further for 1 h. H_2O (8.0 mL) was added to quench the reaction mixture and was then extracted with ethyl acetate (20.0 mL). The organic layer was dried over $MgSO_4$, filtered, and concentrated in vacuo to obtain the crude product. It was washed with pentane (2 × 2.0 mL), and the residue was then extracted by adding toluene (2 × 5.0 mL). The toluene layer was concentrated, and further recrystallization of the residue with diethylether and pentane mixture (2:1) and storing at −30 °C afforded **6** as a light green solid. Single crystals suitable for X-ray diffraction analysis were obtained from slow evaporation by layering of pentane over concentrated solution of the complex in dichloromethane at 0−5 °C. Yield = 30.0 mg, 25%. ^{1}H NMR (500 MHz, CD_2Cl_2, 298 K): δ 6.71 (d, J = 4.5 Hz, 1H), 7.06 −7.12 (m, 3H), 7.16 (t, J = 7.5 Hz, 2H), 7.26 (t, J = 7.5 Hz, 2H), 7.43−7.46 (m, 3H), 7.50 (d, J = 7.5 Hz, 2H), 7.64 (d, J = 7.5 Hz, 1H) 7.90 (td, J = 8.0, 1.5 Hz, 1H), 7.97 (d, J = 5.5 Hz, 1H); ^{13}C{^{1}H} NMR (125 MHz, CD_2Cl_2, 298 K): δ 119.0, 121.4, 124.5, 125.0, 128.5, 128.7, 129.0, 133.1, 134.1, 135.0, 136.3, 140.9, 147.0, 148.8, 161.0, 164.1, 178.9; elemental analysis (%) calculated for $C_{21}H_{16}AuNS$: C, 49.32; H, 3.15; N, 2.74; Found: C, 49.17; H, 3.00; N, 2.80.

***cis*-[(N^C)AuL$_2$] [N^C = 2-(2-thienyl)pyridine, L = C_6F_5] (7).** This reaction was performed according to the general procedure. To iodopentafluorobenzene (151.0 mg, 0.514 mmol) in diethylether (5.0 mL), *n*-BuLi (0.33 mL, 0.537 mmol, 1.6 M soln. in hexanes) was added, and this was transferred to a flask containing **B** (100.0 mg, 0.233 mmol) in diethylether. The crude product thus obtained was purified by flash column chromatography using silica gel (eluent: Hexane/EtOAc = 5/1) to obtain **7** as light yellow solid. Single crystals suitable for X-ray diffraction analysis were obtained from slow evaporation by layering of pentane over a concentrated solution of the complex in diethylether at 0−5 °C. Yield = 61 mg, 38%. IR (KBr): ν_{max} 3414, 2923, 2853, 1738, 1637, 1610, 1509, 1477, 1462, 1365, 1309, 1263, 1163, 1073, 967, 906, 885, 812, 785, 757, 732, 629, 466 cm^{-1}; ^{1}H NMR (500 MHz, $CDCl_3$, 298 K): δ 6.55 (d, J = 4.5 Hz, 1H), 7.24 (td, J = 4.5, 1.5 Hz, 1H), 7.47 (d, J = 5 Hz, 1H), 7.67 (d, J = 8 Hz, 1H), 8.02 (td, J = 6.5, 1.5 Hz, 1H), 8.07 (d, J = 5.5 Hz, 1H); ^{13}C{H} NMR (125 MHz, $CDCl_3$, 298 K): δ 119.7, 122.5, 130.2, 132.0, 137.5 (dm, $^1J_{C-F}$ = 251.0 Hz), 138.0 (dm, $^1J_{C-F}$ = 251.0 Hz), 139.5 (dm, $^1J_{C-F}$ = 251.0 Hz), 142.4, 145.6 (dm, $^1J_{C-F}$ = 250.0 Hz), 146.0, 146.5 (dm, $^1J_{C-F}$ = 250.0 Hz), 149.0, 161.1, 162.4, (note: resonances for 3C submerged in baseline); ^{19}F NMR (376 MHz, $CDCl_3$, 298 K): δ −120.5 (m, 2F, *o*-C_6F_5), −120.6 (m, 2F, *o*-C_6F_5), −156.0 (t, $^3J_{F-F}$ = 18.8 Hz, 1F, *p*-C_6F_5), −156.9 (t, $^3J_{F-F}$ = 18.6 Hz, 1F, *p*-C_6F_5), −160.1 (t, $^3J_{F-F}$ = 18.8 Hz, 2F, *m*-C_6F_5), −161.2 (t, $^3J_{F-F}$ = 19.1 Hz, 2F, *m*-C_6F_5); elemental analysis (%) calcd for $C_{21}H_6AuF_{10}NS$: C, 36.49; H, 0.87; N, 2.03; Found: C, 36.77; H, 0.89; N, 1.97.

***cis*-[N^C = 2-(5-methyl-2-thienyl)pyridine, L = C_6F_5] (8).** This reaction was performed according to the general procedure. To iodopentafluorobenzene (146.3 mg, 0.497 mmol) in diethylether (5.0 mL), *n*-BuLi (0.33 mL, 0.537 mmol, 1.6 M soln. in hexanes) was added, and this mixture was transferred to a flask containing **C** (100.0 mg, 0.226 mmol) in diethylether. The crude product thus obtained after workup was purified by flash column chromatography using silica gel (eluent Hexane/EtOAc = 5:1) to obtain **8** as yellow-green solid. Yield = 90 mg, 56%. Alternatively, direct recrystallization of the crude product using ether and pentane mixture also afforded analytically pure compound. Single crystals suitable for X-ray diffraction analysis were obtained from slow evaporation by layering of pentane over concentrated solution of the complex in diethylether at 0−5 °C. IR (KBr): ν_{max} 3413, 2925, 2027, 1637, 1615, 1508, 1463, 1477, 1366, 1264, 1250, 1160, 1072, 967, 880, 842, 812, 789, 765, 620, 473 cm^{-1}; ^{1}H NMR (500 MHz, CD_2Cl_2, 298 K): δ 2.49 (d, J = 1.0 Hz, 3H), 6.19 (d, J = 1.0 Hz, 1H), 7.13 (td, J = 6.0, 1.5 Hz, 1H), 7.52 (dd, J = 6.0, 1.5 Hz, 1H), 7.95 (td, J = 6.0, 1.5 Hz, 1H), 7.97 (dd, J = 6.0,1.5 Hz, 1H); ^{13}C{^{1}H}NMR (125.MHz, CD_2Cl_2, 298 K): δ 15.4, 119.6, 122.2, 130.6, 137.5 (dm, $^1J_{C-F}$ = 251.6 Hz), 138.0 (dm, $^1J_{C-F}$ = 251.0 Hz), 140.0 (dm, $^1J_{C-F}$ = 251.0 Hz), 143.0, 143.8, 145.0 (dm, $^1J_{C-F}$ = 251.0 Hz), 147.0, 147.1 (dm, $^1J_{C-F}$ = 251.0 Hz), 148.0 (dm, $^1J_{C-F}$ = 251.0 Hz), 149.0, 161.4, 163.0, (note: resonances for 2C submerged in baseline); ^{19}F NMR (376 MHz, $CDCl_3$, 298 K): δ −120.5 (m, 2F, *o*-C_6F_5), −120.6 (m, 2F, *o*-C_6F_5), −156.2 (t, $^3J_{F-F}$ = 18.8 Hz, 1F, *p*-C_6F_5), −157.1 (t, $^3J_{F-F}$ = 21.5 Hz, 1F, *p*-C_6F_5), −160.20 (t, $^3J_{F-F}$ = 18.8 Hz, 2F, *m*-C_6F_5), −161.21 (t, $^3J_{F-F}$ = 22.5 Hz,

2F, *m*-C_6F_5); elemental analysis (%) calcd for $C_{22}H_8AuF_{10}NS$: C, 37.46; H, 1.14; N, 1.99; Found: C, 37.63; H, 1.27; N, 2.06.

Acknowledgment. We thank S. V. Rocha and Dr. N. Finney for help with excited-state lifetime measurements. K.V. is grateful to the University of Zürich and Prof. H. Berke for generous support.

Supporting Information Available: X-ray crystallographic data for complexes **1**−**2** and **4**−**8** in CIF format, absorbance and emission spectra of **4** and **5** (Figure S1), thermogravimetric analysis of **2** and **3** (Figure S2); ORTEP plots of **4**, **6**, and **7** (Figures S3−S5); crystallographic details of all X-ray structures (Tables S1 and S2); and computational details. This material is available free of charge via the Internet at http://pubs.acs.org.